Green Chemistry

Enhanced microbial production of protocatechuate from engineered sorghum using an integrated feedstock-to-product conversion technology

Journal:	*Green Chemistry*
Manuscript ID	GC-ART-05-2023-001481.R1
Article Type:	Paper
Date Submitted by the Author:	12-Jul-2023
Complete List of Authors:	Garcia, Valentina; Joint BioEnergy Institute; Sandia National Laboratories California Pidatala, Venkataramana; Joint BioEnergy Institute, Deconstruction; Lawrence Berkeley National Laboratory Barcelos, Carolina; Lawrence Berkeley National Laboratory; Advanced Biofuels and Bioproducts Process Development Unit Liu, Dupeng; Lawrence Berkeley National Laboratory; Advanced Biofuels and Bioproducts Process Development Unit Otoupal, Peter; Joint BioEnergy Institute; Sandia National Laboratories California, Biomass Science and Conversion Technology Wendt, Oliver; Joint BioEnergy Institute Choudhary, Hemant; Joint BioEnergy Institute, Biomanufacturing and Biomaterials Department; Sandia National Laboratories California Sun, Ning; Lawrence Berkeley National Laboratory, Biological Systems and Engineering Division; Advanced Biofuels and Bioproducts Process Development Unit Eudes, Aymerick; Joint Bioenergy Institute, Emeryville, CA; Lawrence Berkeley National Laboratory Sundstrom, Eric; Lawrence Berkeley National Laboratoty, Advanced Biofuels Process Demonstration Unit; Advanced Biofuels and Bioproducts Process Development Unit Scheller, Henrik; The Joint BioEnergy Institute; Lawrence Berkeley National Laboratory Putnam, Daniel; Joint BioEnergy Institute, LEAD; University of California Davis, Department of Plant Sciences Mukhopadhyay, Aindrila; Joint BioEnergy Institute; Lawrence Berkeley National Laboratory Gladden, John; Joint BioEnergy Institute; Sandia National Laboratories California Simmons, Blake; Joint BioEnergy Institute; Lawrence Berkeley National Laboratory Rodriguez, Alberto; Joint BioEnergy Institute; Sandia National Laboratories California,

ARTICLE

Received 00th January 20xx,
Accepted 00th January 20xx

DOI: 10.1039/x0xx00000x

Enhanced microbial production of protocatechuate from engineered sorghum using an integrated feedstock-to-product conversion technology

Valentina E. Garcia [1,2], Venkataramana Pidatala [1,3], Carolina A. Barcelos [3,4], Dupeng Liu [3,4], Peter Otoupal [1,2], Oliver Wendt [1], Hemant Choudhary [1,5], Ning Sun [3,4], Aymerick Eudes [1,6], Eric Sundstrom [3,4], Henrik V. Scheller [1,6], Daniel H. Putnam [1,7], Aindrila Mukhopadhyay [1,3], John M. Gladden [1,2], Blake A. Simmons [1,3] and Alberto Rodriguez [1,2*]

Building a stronger bioeconomy requires production capabilities that are largely generated through microbial genetic engineering. Plant feedstocks can additionally be genetically engineered to generate desirable feedstock traits and provide precursors for direct microbial conversion into desired products. The oleaginous yeast *Rhodosporidium toruloides* is a promising organism for this type of conversion as it can grow on a wide range of deconstructed biomass and consume a variety of carbon sources. Here, we leveraged *R. toruloides* native *p*-coumaric acid consumption pathway to accumulate protocatechuate (PCA) from 4-hydroxybenzoate (4HBA) released from a sorghum feedstock line genetically engineered to overproduce 4HBA. We did so by generating and evaluating an *R. toruloides* strain that accumulates PCA, *RS*Δ12623. We then show that at two scales a cholinium lysinate pretreatment with enzymatic saccharification successfully extracts 95% of the 4HBA from the engineered sorghum biomass while producing deconstructed lignin that can be more efficiently depolymerized in a subsequent thermochemical reaction. We also demonstrate that strain *RS*Δ12623 can convert more than 95% of 4HBA to PCA while consuming >95% of the glucose and >80% of the xylose present in sorghum hydrolysates. Finally, to evaluate the scalibility of such fermentations, we conducted the conversion of 4HBA to PCA in a 2 L bioreactor under controlled conditions. This work demonstrates the potential of purposefully producing aromatic precursors *in planta* that can be liberated during biomass deconstruction for direct microbial conversion to desirable bioproducts.

1 Joint BioEnergy Institute, Emeryville, CA 94608, USA.
2 Department of Biomaterials and Biomanufacturing, Sandia National Laboratories, Livermore, CA 94550, USA.
3 Biological Systems and Engineering Division, Lawrence Berkeley National Laboratory, Berkeley, CA, 94720, USA.
4 Advanced Biofuels and Bioproducts Process Development Unit, Emeryville, CA, 94608, USA.
5 Department of Bioresources and Environmental Security, Sandia National Laboratories, Livermore, CA 94550, USA.
6 Environmental Genomics & Systems Biology Division, Lawrence Berkeley National Laboratory, Berkeley, CA, 94720, USA.
7 Department of Plant Sciences, University of California, Davis, CA, 95616, USA.
**Corresponding author: Alberto Rodriguez*
Email: alberto@lbl.gov

Introduction

Synthetic biology unlocks the ability to generate innumerable bioproducts in an environmentally friendly manner.[1] Microbial production strains can be obtained by introducing novel metabolic pathways into amenable organisms or by modifying native pathways in metabolically attractive hosts.[2] Just as important as the microbes used for fermentation and conversion are the feedstocks they are paired with for fueling biosynthesis.[3] Lignocellulosic biomass is a globally distributed and sustainable energy source that can be deconstructed into streams containing primarily C6 and C5 sugars that can serve as microbial substrates.[4]

To generate microbial feedstocks from lignocellulosic biomass, the biomass is usually chemically pretreated to partially depolymerize or solubilize the polysaccharides cellulose and hemicellulose, which can then be enzymatically hydrolyzed to monomeric sugars.[5] Common chemical pretreatment methods include mixing the biomass with acid, alkali, ammonia, organic solvents, or ionic liquids, and allowing them to react at high temperatures.[6] Decades of research have shown that the pretreatment solvent, biomass type, and reaction conditions strongly influence the depolymerization efficiency and the types of compounds that can be released from the biomass.[6,7] Another main component of lignocellulosic biomass is lignin, a structurally complex and recalcitrant polymer that is synthesized in plants from monomeric aromatic compounds.[8] High molecular weight lignin is typically removed after pretreatment,[9] but aromatic compounds like *p*-hydroxycinnamic acids that are attached by ester linkages to lignin or hemicellulose in grassy biomasses, such as corn or sorghum, can be released in the hydrolysates.[10,11]

Sorghum, in particular, is an important source of lignocellulosic biomass with many features that make it an attractive renewable crop, such as high biomass yields, high water use efficiency, drought tolerance, and genetic tractability.[12] The ability to genetically engineer a bioenergy crop presents an opportunity to tailor the plant composition such that it improves the economics of biorefineries, for example by modifying the cell wall to increase saccharification yields, reducing the lignin content, and accumulating specific products *in planta*.[13,14] While some *in planta* accumulated products may hold significant value on their own,[15,16] others could act as precursors for microbial conversion. However, this union of engineered biomass with engineered conversion hosts has yet to be demonstrated.

The oleaginous and carotenogenic yeast *Rhodosporidium toruloides* is an attractive production host for the bioconversion of lignocellulosic biomass. Found in nature on recalcitrant materials such as wood pulp and grasses, *R. toruloides* is well adapted to grow in the presence of various microbial inhibitors found in lignocellulosic hydrolysates.[17,18] Additionally, it is able to consume a wide array of carbon sources, including glucose, xylose, and lignin-derived aromatics such as *p*-coumaric acid.[19] Many synthetic biology techniques, including *Agrobacterium tumefaciens*-mediated transformation and CRISPR/Cas9-mediated gene knockouts, have been applied in *R. toruloides* to manipulate its metabolic pathways and promote the biosynthesis of different compounds from lignocellulosic biomass.[20,21] Recently, a multi-omics metabolic model of *R. toruloides* has been constructed that details the *p*-coumaric acid utilization pathway.[22] Many of the predicted metabolic intermediates, including 4-hydroxybenzoate (4HBA), protocatechuate (PCA), and beta-ketoadipate, reflect the *p*-coumaric acid degradation pathways observed in bacterial systems[22–25] and are themselves interesting compounds for bioproduction.[26–28] Knocking out genes that are predicted to code for enzymes within the *p*-coumaric acid utilization pathway should generate *R. toruloides* strains with the ability to accumulate these intermediates.

PCA is a known antioxidant with many potential pharmacological applications, including anti-inflammatory and anti-viral properties[27,29] that can also be used as a platform molecule to generate other industrially relevant chemicals, such as muconate and 2-pyrone-4,6-dicarboxylate.[30–32] Additionally, only one enzyme in *R. toruloides* is predicted to catabolize PCA, [22] making it an ideal knockout target for demonstrating *R. toruloides* capabilities to accumulate bioproducts derived from *p*-coumaric acid and 4HBA. The enzyme, RTO4_12623,[22] is a putative dioxygenase containing an intradiol ring-cleavage dioxygenase domain similar to those present in other PCA 3,4-dioxygenases that utilize iron to cleave aromatic rings and incorporate two oxygen atoms into the substrate molecule.

Currently, bacterial systems have been able to produce titers of PCA up to 9.6 g/L from xylose with *Corynebacterium glutamicum* [33] and up to 21.7 g/L from glucose with *Pseudomonas putida*[34]; however, these former studies use synthetic media containing large quantities of pure sugars as their carbon sources. As lignocellulosic biomass is a renewable carbon source that could contain the aromatic precursors to PCA, using a lignocellulosic based feedstock would provide a more sustainable option for PCA production. Additionally, when paired with an appropriate microorganism capable of growing in lignocellulosic hydrolysates and *p*-coumaric acid, such as *R. toruloides*, minimal genetic engineering of the conversion host should be required.

Recently, sorghum lines were engineered to overproduce and accumulate the immediate precursor to PCA, 4HBA. This was done by expressing two enzymes from *E. coli* in plastids, a chorismate pyruvate-lyase (UbiC) and a feedback-resistant 3-deoxy-D-arabino-heptulosonate-7-phosphate synthase (DAHPS), to increase carbon flux to the shikimate pathway and redirect the chorismate pool to the synthesis of 4HBA. In field trials the 4HBA sorghum lines accumulated 4HBA at levels higher than 1% of their dry biomass weight while only reducing biomass yields by 11-15% compared to the wild type.[27]

Ionic liquids are considered attractive biomass pretreatment solvents because of their ability to partially solubilize lignocellulosic components, promoting cellulose digestibility and enhancing lignin removal and recovery.[35] Considering that the ionic liquid cholinium lysinate ([Ch][Lys]) has proven to be effective at deconstructing sorghum biomass and generating hydrolysates compatible with fermentation by *R. toruloides,*[36] we hypothesized that [Ch][Lys] pretreatment with saccharification can be applied to efficiently release fermentable sugars and 4HBA from the

engineered sorghum. The resulting hydrolysate combined with an *R. toruloides* strain carrying an RTO4_12623 knockout is expected to produce PCA. This would not only be the first demonstration of PCA accumulated from lignocellulosic hydrolysates, but it would also be the first demonstration of microbial conversion of a genetically enriched aromatic into a bioproduct using a biocompatible ionic liquid-based deconstruction process. To test this possibility here, we 1) constructed and verified an RTO4_12623 knockout strain of *R. toruloides*, 2) generated and characterized hydrolysates from wild-type and 4HBA-enriched biomass, 3) evaluated the ability of the *R. toruloides* strain to grow and accumulate PCA in the generated hydrolysates, and 4) investigated the robustness of the process by increasing the pretreatment reaction scale and the bioreactor size during bioproduction.

Experimental

Chemicals

All chemicals were obtained from Sigma-Aldrich (St. Louis, MO, USA) unless otherwise indicated. Cholinium lysinate was obtained from Proionic (Grambach, Styria, Austria). Commercial cellulase (Cellic CTec3) and hemicellulase (Cellic HTec3) enzymes were provided by Novozymes (Franklinton, NC, USA). The PvuII restriction enzyme, salmon sperm DNA, and YNB without amino acids were obtained from Thermo Fisher Scientific (Waltham, MA, USA). Cefotaxime was obtained from TCI Chemicals (Portland, OR, USA) and carbenicillin was obtained from Alfa Aesar (Tewksbury, MA, USA). BD Difco YPD was purchased from Fisher Scientific (Waltham, MA, USA).

Sorghum growth, harvesting, and storage

The engineered 4HBA overproducing sorghum (line Eng-2) used in this work has been previously described.[37] Engineered plants and wild-type segregant control (variety BTx430) in the T3 generation were cultivated at the University of California Davis Plant Sciences Research Farm in 2021. Growth conditions have been previously documented.[37] For each genotype, plants from an entire four-row plot (3 × 6 m) were harvested without their panicles using a Wintersteiger Cibus forage chopper (Wintersteiger, Salt Lake City, UT) and dried down in the field. Dried chopped biomass was further milled using a Model 4 Wiley Mill equipped with a 2 mm screen mesh (Thomas Scientific, Swedesboro, NJ).

Biomass compositional analysis

The glucan, xylan, lignin, and 4HBA content of untreated sorghum was determined using the two-step acid hydrolysis procedure described by the National Renewable Energy Laboratory.[38] During the experiments, 300 mg of extractive-free biomass was exposed to 3 mL of 72% w/w H_2SO_4 for 1 h at 30 °C, followed by a second hydrolysis in 4% w/w H_2SO_4 for 1 h at 121 °C. The hydrolysate was spectrophotometrically analyzed for acid-soluble lignin or ASL (NanoDrop 2000; Thermo Fisher Scientific, Waltham, MA) using the absorbance at 240 nm. The concentrations of monomeric sugars (glucose and xylose) and 4HBA were determined by HPLC as detailed below. After the two-step acid hydrolysis, acid insoluble lignin was obtained by filtering the hydrolysates through filter crucibles. Acid insoluble lignin (AIL) was determined by subtracting the weight of oven-dried residual solids (105 °C) and the ash content (575 °C).

Hydrolysate generation

Biomass pretreatment was carried out at a solid loading of 15 wt.% in a one-pot configuration using a 1 L Parr reactor (Parr Instrument Company, model: 4555-58, Moline, IL, USA), 10 wt.% [Ch][Lys] and 75 wt.% water. Typically, 60 g of biomass was mixed thoroughly with 40 g of [Ch][Lys] and 300 g of water followed by heating at 140 °C for 3 h. Post pretreatment, 10 M HCl was added to adjust the pH of the biomass slurry to 5. Subsequently, a commercial enzyme mixture, Cellic CTec3 and HTec3 (9:1 v/v), was added to the biomass slurry at a concentration of 10 mg enzyme/g biomass to carry out saccharification at 50 °C for 72 h at 48 rpm in the same Parr vessel. Scale-up experiments were carried out in a 10 L Parr vessel (Parr Instrument company, model: 4556, Moline, IL, USA) using 900 g of biomass, 600 g of [Ch][Lys] and 4500 g of water under otherwise identical conditions. After hydrolysis, liquid samples were collected and centrifuged at 8,000 rpm for 20 min and the supernatant was filtered using 0.45 µm Rapid flow centrifuge filters (Nalgene, USA) for HPLC analysis.

Calorimetric evaluation

The energy content of untreated and hydrolyzed biomass was measured using an oxygen bomb calorimeter (IKA C2000, Wilmington, NC, USA). The details of the setup and procedure have been described previously.[39] Briefly, the biomass samples were dried and pressed into pellet form using a hydraulic pelletizer (MTI 12T pelletizer, Richmond, CA, USA). The bomb calorimeter was calibrated using a known amount of standard benzoic acid (Sigma-Aldrich, St. Louis, MO, USA). The weight loss of the pelletized samples and the temperature rise in the calorimeter were recorded after combustion. The energy density of solid samples was calculated using the following equation:

$$ED = ED_{std} \times \frac{W_{std} \times \Delta T_{sample}}{W_{sample} \times \Delta T_{std}}$$

where ED is energy density of sample, ED_{std} is the energy density of standard benzoic acid, W_{std} and W_{sample} represent the weight loss of standard benzoic acid and biomass samples, respectively. ΔT_{std} and ΔT_{sample} are the temperature rise recorded after combustion of standard benzoic acid and biomass samples, respectively.

Residual solids (lignin-rich material) analysis

The quality analysis of the residual solids containing lignin was performed in terms of ease of depolymerization under milder oxidative conditions as follows. Typically, residual solids, polyoxotungstate catalyst, oxidant, and water were mixed in a ratio of 5:2:3:90 (w/w), pressurized with 20 bar N_2 and heated at 140 °C for 1 h. Unreacted solids were separated from the aqueous stream containing depolymerized products by centrifugation. The solids were washed with water and lyophilized. Gel permeation chromatography (GPC) was used to determine the relative molecular weight distribution of lignin in substrate (residual solids) and unreacted solids after the depolymerization reaction. GPC was performed on a Tosoh Ecosec HLC-8320GPC (Griesheim, Germany) equipped with Agilent PLgel 5 µm Mixed-D and a diode array detector as described previously [40]. The aqueous stream containing depolymerized products, after dilution and filtration through Thermo Scientific Nalgene Syringe Filter (0.45 µm SFCA), was analyzed using an Agilent HPLC 1260 infinity system (Santa Clara, California, United States) equipped with a Bio-Rad Aminex HPX-87H column and a refractive index detector at 35 °C. An aqueous solution of H_2SO_4 (4 mM) was used as the eluent (0.6 mL min^{-1}, column temperature 60 °C).

***Rhodosporidium toruloides* strain engineering**

The software sgRNA Scorer 2.0[41] was used to identify potential guide sequences targeting early exons in RTO4_12623. The target sequence used to generate the RTO4_12623 knockout ("AGGGAGAGACGCACCGAGGG") was cloned into plasmid pPBO.078 (generating pRS-Cas9_12623) to randomly integrate Cas9 and the guide RNA into the genome of *R. toruloides*. For transformation, pRS-Cas9_12623 was linearized by digestion with PvuII. Wild-type *R. toruloides* IFO0880, was streaked onto YPD plates, individual colonies were selected, and grown in 10 mL YPD overnight at 30 °C with 200 RPM shaking. The following afternoon, cultures were diluted to an OD_{600} such that they would reach an OD_{600} of 0.8 the following morning, assuming a growth rate of 0.3 h^{-1}. Cultures for transformation were pelleted at 4,000 g for 5 min and washed twice with water and twice with 150 mM LiAc. Pellets were resuspended in 240 µL 50% (wt/vol) PEG 4000, 54 µL 1.0 M LiAc, 10 µL salmon sperm DNA, and 56 µL of linearized DNA (approximately 1 mg total DNA). Cells were incubated at 30 °C for 1 h, supplemented with 34 µL of DMSO, and incubated at 37 °C for 5 min. Cells were centrifuged, washed once with YPD, and grown overnight in 2 mL YPD. Overnight cultures were plated on YPD supplemented with G418 and grown for 2-3 d at 30 °C. Resulting colonies were screened in YPD supplemented with 4 g/L of *p*-coumaric acid. Knockouts were initially identified by the changing color of YPD to a dark brown, indicating PCA production, and confirmed by PCR (forward primer: ACTCGAATACAACCATGCGGA; reverse primer: GTACTTTGCGATCTTGGGCG).

The wild-type RTO4_12623 sequence from *R. toruloides* IFO0880 driven off of a Acp1 promoter in VEG22 which was transformed into wild-type *R. toruloides* IFO0880 and *RS*Δ12623 by *Agrobacterium*-mediated transformation. 100 ng of plasmid VEG22 was electroporated into *Agrobacterium tumefaciens* AGL-1 in 10% glycerol with a 1250 V, 25 uF capacitance, 400 ohms resistance pulse using a Bio-Rad Gene Pulser Xcell Electroporation system. Cells were recovered with 1 mL of SOC media then plated on LB plates with 50 µg/mL kanamycin and placed at 30 °C for 48 h. Colonies from the pRS-WT12623 transformed *Agrobacterium*, wild-type *R. toruloides*, and *RS*Δ12623 were picked and grown overnight in SOC medium or YPD. *Agrobacterium* cells were then diluted to an OD_{600} of 0.2 with SOC containing 1 mM acetosyringone and the *R. toruloides* strains were diluted to an OD_{600} of 0.2 in YPD. When the *R. toruloides* cultures reached an OD_{600} of ~1, 0.06 OD*mL of *R. toruloides* was mixed with 0.6 OD*mL of *Agrobacterium*, pelleted, and resuspended in 300 µL liquid induction medium. This mixture was then plated on induction plates and incubated at 25 °C for 2-3 d. The co-cultures were then resuspended in 1 mL YPD and spun at 2000 g for 20 sec. The supernatant was removed and the *R. toruloides* pellet was plated on YPD plates containing 300 µg/mL cefotaxime, 300 µg/mL carbenicillin, and 100 µg/mL nourseothricin. Plates were incubated at 30 °C for 2 d, and colonies were picked into 1 mL YPD and grown at 30 °C overnight then were screened for PCA accumulation.

To assess PCA accumulation from *p*-coumaric acid, WT *R. toruloides*, *RS*Δ12623, and both transformed with VEG 22 were inoculated at a starting OD_{600} of 0.1 in 48-well flower plates in 1 mL YPD with or without 4 g/L *p*-coumaric acid. To assess PCA consumption, WT *R. toruloides* and *RS*Δ12623 inoculated at a starting OD_{600} of 0.1 in 48-well flower plates in 1 mL YNB with 4 g/L PCA. All flower plates were incubated at 30 °C shaking at 999 rpm in a humidified Multitron (Infors). Full wells were taken every two days up to day 6. Production experiments were performed three times in triplicate while consumption experiments were performed twice in triplicate, except for the no cells condition which was performed in duplicate.

The strains produced for this study are archived at the Joint BioEnergy Institute under the following names: pRS-Cas9_12623 (JBx_238463), VEG22 (JBx_238464), RSΔ12623 (JBx_238466), WT+VEG22 (JBx_238465), and RSΔ12623 + VEG22 (JBx238467).

Inoculum cultivation and batch fermentations

Inocula cell growth was performed in two steps. The first seed culture was grown in 250 mL baffled flasks containing 50 mL of YPD media. A 10% (v/v) inoculum size was used to inoculate the second seed culture, using a 50:50 mixture of YPD and filtered hydrolysate. In both steps, cells were incubated at 30 °C and 200 rpm for 24 h. Microbial growth was measured by optical density at 600 nm via a spectrophotometer.

Shake flask fermentations were performed in 125 mL shake flasks with a final volume of 25 mL to compare the production of PCA by wild-type and *RS*Δ12623 strains in both wild-type and 4HBA sorghum hydrolysates. Each combination was performed in triplicate. The flasks were inoculated to have an OD of 0.5 and shaken at 200 rpm at 30 °C for 7 d. The fermentations were sampled daily over the course of 7 d by transferring 300 µL from each flask to a 96-well plate. The plate was spun at 4000 g for 2 min and the supernatant was transferred and stored at -20 ºC for HPLC analysis detailed below. The cell pellets were washed with 1 mL of water and resuspended in 300 µL of water before measuring the

OD_{600}. The OD_{600} was taken using a 96-well plate on the Spectra max Plus 384 microplate reader (Molecular Devices).

Batch fermentations were also performed in 2 L Sartorius bioreactors (Sartorius Stedim, Göttingen, Germany) using filtered wild-type and 4HBA hydrolysates and *RS*Δ12623. Each vessel was batched with 900 mL of filtered hydrolysate, 100 mL of cells from the second seed culture and 250 mL of Durasyn 164, to a final volume of 1.25 L. Dissolved oxygen was controlled at 30% saturation by varying agitation from 300–1000 rpm. The OD_{600} for these experiments were taken in cuvettes using the GENESYS 10S UV–Vis (Thermo Scientific). Statistical analysis and graphs were generated using GraphPad Prism.

Metabolite quantification

For quantifying 4HBA and PCA concentrations, collected samples were centrifuged at 15,000 g for 2 min. The supernatant was diluted 1:20 in water and filtered through a 0.45 µm polypropylene filter plate (Agilent 200984-100). The samples were analyzed, similarly to previously described[42] on a 1260 Infinity II (Agilent Technologies) equipped with an Eclipse Plus Phenyl-Hexyl column (250 mm length, 2.6 mm diameter, 5 µm particle, Agilent Technologies, 95990-912), and a UV detector. Two mobile phases were used, 10 mM ammonium acetate with 0.07% formic acid in water (Solvent A) and 10 mM ammonium acetate with 0.07% formic acid in 90% acetonitrile (Solvent B). The profile mixture was as follows: 30% Solvent B, 0.5 mL/min for 12 min, 80% Solvent B, 0.5 mL/min for 0.1 min, 100% Solvent B, 0.5 mL/min for 0.5 min, 100% Solvent B, 1.0 mL/min for 0.2 min, and 30% Solvent B, 1.0 mL/min for 2.8 min. The column temperature was kept at 50 °C. *p*-Coumaric acid concentrations were compared against analytical standards at a 254 nm spectral profile. 4HBA concentrations were compared against analytical standards at a 280 nm spectral profile and PCA concentrations were compared against analytical standards at a 310 nm spectral profile.

For sugar analysis, collected samples were centrifuged at 15,000 g for 2 min. The supernatants from the initial 3 time points were diluted 1:10 and subsequent timepoints were diluted 1:3 in water. All timepoints were then filtered through a 0.45 µm polypropylene filter plate (Agilent 200984-100). Glucose and xylose were quantified as previously published[36] with an Agilent Technologies 1200 series HPLC system equipped with an Aminex HPX-87H column (BioRad Laboratories, USA), and a refractive index detector. The column was kept at 60 °C during analysis. 4 mM H_2SO_4 was used as a mobile phase with a flow rate of 0.6 mL/min and 5 µL sample injection volumes. The concentrations of interest were calculated by comparison of peak areas to standard curves made with pure compounds. Initial 4HBA and sugar concentrations were determined by analyzing the same hydrolysate samples in triplicate. The percent theoretical yield was calculated by dividing the molarity of PCA by the molarity of 4HBA in the initial hydrolysates. Graphs were generated using Prism (GraphPad).

Results and Discussion

Construction of an *R. toruloides* strain that accumulates PCA

R. toruloides can consume *p*-coumaric acid as a carbon source in defined media or complex plant hydrolysates.[18] As part of the *p*-coumaric acid utilization model, PCA is processed by RTO4_12623, a predicted dioxygenase.[22] To validate the role of RTO4_12623 in *p*-coumaric acid utilization, RTO4_12623 was knocked out using CRISPR/Cas9 to generate the strain *RS*Δ12623. In rich (YPD) medium supplemented with 4 g/L *p*-coumaric acid, wild-type *R. toruloides* and *RS*Δ12623 reached an OD_{600} of 4.19 ± 1.48 and 5.62 ± 0.30 respectively, and both consumed >90% of the *p*-coumaric acid within 6 days (Fig. 1A). *RS*Δ12623 accumulated 1.53 ± 0.31 g/L of PCA while the wild-type strain produced no detectable PCA (Fig. 1B). In YPD without *p*-coumaric acid, *RS*Δ12623 accumulated low and variable amounts of PCA, 64 ± 50 mg/L, indicating that the vast majority of the PCA produced by *RS*Δ12623 when fed *p*-coumaric acid was derived from the supplied *p*-coumaric acid and not an alternative metabolic pathway. When a wild-type copy of RTO4_12623 was reintroduced into *RS*Δ12623 by transforming it with the plasmid VEG22, PCA accumulation was nearly eliminated in both YPD and YPD supplemented with 4 g/L *p*-coumaric acid (Fig. 1B). Additionally, as *RS*Δ12623 does not have an intact *p*-coumaric acid utilization pathway, it failed to grow in a defined medium (YNB) with PCA as sole carbon source (Fig. 1C) and there was no significant consumption of PCA over 6 days of fermentation (Fig. 1D). Together this shows that RTO4_12623 plays a key role in the *p*-coumaric acid utilization pathway and by deleting this step *R. toruloides* can stably accumulate PCA from *p*-coumaric acid that is measurable in the culture medium.

Generation and characterization of hydrolysates and residual solids

Recently, the bioenergy crop sorghum was engineered to overproduce and accumulate 4HBA, the predicted precursor to PCA in the *R. toruloides p*-coumaric acid consumption pathway.[37] This engineered feedstock provides an opportunity to obtain 4HBA-enriched hydrolysates for fermentation with the strain *RS*Δ12623 to produce PCA. A proven method for generating sugar-rich hydrolysates from sorghum is an ionic liquid-based ([Ch][Lys]) deconstruction process performing thermochemical pretreatment and enzymatic saccharification in the same vessel.[36] This process consolidates the unit operations of feedstock deconstruction to reduce costs while still generating hydrolysates that have shown to be compatible with *R. toruloides* growth after pH adjustment and nitrogen supplementation.[21,43,44] However, these studies have focused on tracking the conversion of sugars and it is not known if aromatic compounds are also efficiently released from biomass. In the case of 4HBA sorghum, this aromatic compound is expected to be present in extractives in the form of glucose conjugates (presumably stored in vacuoles) and ester-bound to the cell wall.[37] Here we investigate the impact that 4HBA-enriched biomass may have on the composition of hydrolysates, residual lignin-containing solids, and the fermentation capabilities of *R. toruloides*, when subjected to this [Ch][Lys] conversion process. A scheme of the complete process is presented in Figure 2.

Prior to performing biomass deconstruction reactions, a compositional analysis of field-grown wild-type and 4HBA biomass samples was conducted to determine the contents of the starting materials. This analysis revealed a slightly (8%) higher glucan content in 4HBA biomass compared to wild-type (Table 1). Additionally, the 4HBA biomass contained substantially (55%) higher acid-soluble lignin contents, likely due to the increased 4HBA accumulation in this genotype, while the xylan and acid-insoluble lignin contents remained unchanged (Table 1). A sulfuric acid extraction on the initial biomasses showed that the engineered biomass contained 1.4 ± 0.03 % 4HBA on a dry weight basis while there was no detectable 4HBA in the wild-type biomass.

To determine the effects of the chemical and enzymatic treatments on the composition of the resulting hydrolysates while also attempting to produce high concentrations of consumable substrates, 15% biomass loading was used for pretreatment and saccharification in a 1 L reactor. At this stage, the concentrations of glucose, xylose, and 4HBA in the hydrolysates were determined and used to calculate their deconstruction efficiency from lignocellulosic components. As expected from the initial compositional analysis, the 4HBA hydrolysates contained a much higher concentration of 4HBA, up to 2.26 ± 0.40 g/L, compared to the wild-type hydrolysates (Table 2). In terms of conversion percentages, both hydrolysates contained comparable amounts of glucose and xylose. The glucose yield from total glucan was close to 74% for both biomasses and the xylose yield from xylan was only slightly higher in the 4HBA hydrolysates compared to the wild-type hydrolysates (61.55 ± 1.94 vs. 55.58 ± 1.46 %, respectively). Finally, 95.00 ± 5.45 % of the 4HBA present in the 4HBA sorghum biomass was successfully released.

Next, we studied the effect of scaling up the pretreatment and enzymatic hydrolysis by performing a 6-kg reaction in a 10 L pressure vessel under otherwise identical conditions. The amount of material produced at this scale will provide sufficient hydrolysate for fermentations in bioreactors. The 10 L scale yielded similar results to the 1 L reactions with hydrolysates prepared at both scales containing similar amounts of glucose and xylose (Table 2). Across all conditions there was an average glucose conversion of 72% and an average xylose conversion of 63%. This demonstrates that the one-pot reaction with 10% [Ch][Lys] and enzymatic hydrolysis results in high sugar yields, is effective at releasing 4HBA from biomass, and is scalable.

Table 1. Composition of wild-type (WT) and 4HBA enriched sorghum obtained from raw biomass or solids recovered after pretreatment and saccharification. ASL = Acid-soluble lignin. AIL = Acid-insoluble lignin.

Sorghum type	Glucan %	Xylan %	ASL %	Ash content %	AIL %
WT biomass	25.36 ± 0.20	13.30 ± 0.05	4.55 ± 0.04	11.06 ± 0.05	13.77 ± 0.76
4HBA biomass	27.36 ± 0.28	13.63 ± 0.24	7.04 ± 0.07	8.79 ± 0.27	13.42 ± 0.01
WT solids post pretreatment and saccharification	8.98 ± 0.33	1.77 ± 0.05	6.50 ± 0.70	29.30 ± 0.51	24.92 ± 0.62
4HBA solids post pretreatment and saccharification	2.36 ± 0.05	1.10 ± 0.01	6.60 ± 0.59	30.46 ± 0.33	24.93 ± 1.76

Table 2. Composition of hydrolysates generated at different pretreatment scales. Numbers show average ± standard deviation.

Scale	Sorghum type	Glucose (g/L)	Glucose yield (% of glucan)	Xylose (g/L)	Xylose yield (% of xylan)	4HBA (g/L)
1 L	WT	31.50 ± 0.80	74.53 ± 1.89	12.6 ± 0.33	55.58 ± 1.46	0.05 ± 0.00
	4HBA	33.55 ± 0.95	73.68 ± 2.09	14.3 ± 0.45	61.55 ± 1.94	2.26 ± 0.40
10 L	WT	31.45 ± 1.60	70.27 ± 3.57	16.06 ± 0.56	68.43 ± 2.39	0.05 ± 0.00
	4HBA	33.13 ± 2.92	68.62 ± 6.05	15.53 ± 0.82	64.57 ± 3.41	2.45 ± 0.29

The solids obtained after pretreatment and saccharification at 1 L scale were also analyzed to correlate their composition with the hydrolysates. As expected, solids from both wild-type and 4HBA sorghum contained low amounts of polysaccharides and were enriched in lignin after one-pot pretreatment and saccharification (Table 1). Consistent with a higher concentration of glucose in 4HBA versus wild-type sorghum hydrolysates, the post-pretreatment solids from 4HBA sorghum also contained a lower proportion of residual glucan, signalling that the feedstock engineering efforts to accumulate 4HBA also facilitated glucose release with our process (Table 1). The energy density of the 4HBA sorghum prior to deconstruction was found to be similar to that of the wild-type sorghum, as expected due to their comparable lignin, hemicellulose, and ash concentrations (Table 3). Following hydrolysis, the residual solids of 4HBA sorghum exhibited an energy density exceeding that of the wild-type sorghum by 10%. This increase could be attributed to the higher glucan content in the treated wild-type sorghum, as previous research has indicated a negative correlation between glucan concentration and energy density in ionic liquid-pretreated biomass.[16]

Table 3. Calorimetric evaluation of raw wild-type (WT) and 4HBA feedstocks or the solids obtained after pretreatment at a 10 L scale. Numbers show average ± standard deviation.

Sorghum type	Energy density (J/g)	Residual solids (%)
WT raw biomass	15366 ± 216	7.67 ± 2.61
4HBA raw biomass	15637 ± 223	12.71 ± 4.11
WT solids post pretreatment and saccharification	13934 ± 196	38.68 ± 0.38
4HBA solids post pretreatment and saccharification	15373 ± 246	38.23 ± 1.29

The acid-insoluble lignin content in the residual solids from both wild-type and 4HBA sorghum was 25%, as shown in Table 1. The importance of utilization of all major polymeric constituents in lignocellulosic biomass has been stressed for a potential sustainable future biorefinery.[45] Typically, pretreatment of lignocellulosic biomass can also alter the content, structure, and molecular weight of the lignin present, the extent of which is determined by the severity of the pretreatment and, in the case here, the nature and types of ions in the ionic liquid. As a result, lignin in the residual solids along with various chemical impurities may have a complex non-uniform structure and unique or limited chemical reactivity. Hence, it is important to compare the quality of the lignin in the residual solids generated after holocellulosic conversion between the wild type and 4HBA sorghum.

We first investigated the molecular weight distribution of the lignin in residual solids after [Ch][Lys] pretreatment and enzymatic saccharification of wild-type and 4HBA sorghum. The pretreatment of WT and engineered sorghum with aqueous [Ch][Lys] minimized the recondensation of lignin affording lower MW lignin fractions (<1000 Da) in higher abundance compared to higher MW lignin fractions (between 1000-20,000 Da). The molecular weight of lignin in grassy biomass, such as sorghum, is typically lower compared to other lignocellulosic sources like woody biomass.[46] Although similar weight average (M_w ~750-780 Da) and number average (M_n ~205-235 Da) molecular weights were observed for both solids here, solids from 4HBA sorghum had higher polydispersity index (PDI ~3.6) due to an increased concentration of smaller molecular weight fragments (Table 4 and Fig. 3).

The convertibility of these solids under oxidative conditions was then studied as described in the methods. Interestingly, a higher percentage of solids from wild-type sorghum (74.9% conversion) were depolymerized compared to solids from 4HBA sorghum (70.6% conversion) when mixed with polytungstate catalyst in the presence of aqueous hydrogen peroxide. An aqueous stream containing dissolved or depolymerized molecules was analyzed with an HPLC to realize the differences in reactivity from these two residual sorghum solids. Carboxylic acids including formic, oxalic, and acetic acids were observed as the major product from both residual solids. About 70% improvement in the total carboxylic acid yield was observed for the 4HBA solids (400.7 mg of total acids per g of lignin in solids) over wild-type solids (237.1 mg of total acids per g of lignin in solids) under the oxidative conditions employed for lignin depolymerization (Fig. 3). The unreacted solids (<25 wt.% of the residual solids after glucan/xylan utilization) obtained after depolymerization reaction of 4HBA sorghum solids were less polydisperse and had lower M_w and M_n compared to the wild-type sorghum solids (Table 4). Together these results further establish that the sorghum engineered to accumulate 4HBA aids in obtaining lignin that can be easily depolymerized and, therefore, improves the potential of a sustainable biorefinery.

Conversion of 4HBA in sorghum hydrolysates to PCA by strain *RS*Δ12623

After demonstrating that 4HBA can be released alongside monomeric sugars from engineered sorghum biomass, we tested the capacity of *RS*Δ12623 to produce PCA in the hydrolysates. *R. toruloides* wild-type and *RS*Δ12623 strains were first grown on wild-type and 4HBA hydrolysates obtained at the 1 L scale. In preparation for microbial growth, the pH of the generated hydrolysates was adjusted to 7.0, filtered, and supplemented with a final concentration of 5 g/L ammonium sulfate as the nitrogen source required for microbial fermentation.

In 25 mL flask cultures, the wild-type and *RS*Δ12623 strains successfully grew on both wild-type and 4HBA hydrolysates, reaching maximum cell density after 6 or 7 days (Fig. 4A). In all combinations, >95% of the glucose was consumed within 5 days (Fig. 4B) and >80% of xylose was consumed within 7 days (Fig. 4C). In the 4HBA containing hydrolysates, >95% of 4HBA was consumed or converted to PCA (Fig. 4D). Interestingly, 4HBA was converted at the same rate by wild-type and *RS*Δ12623 strains suggesting that neither the disruption of the *p*-coumaric acid pathway nor the metabolic fate of the carbon in 4HBA influence the 4HBA

consumption rate under these conditions. In all cases, glucose appeared to be the preferential carbon source leading to higher xylose and 4HBA consumption after day 3 when most of the glucose was consumed. This effect is consistent with other reports using the same parent strain in different plant hydrolysates containing glucose and xylose[47,48], and the catabolic repression by glucose on alternative sugars and aromatics observed in other fungal and bacterial species.[49–51]

Since 4HBA consumption does not begin until glucose, and potentially xylose, is limited, PCA production does not noticeably occur at the onset of the fermentation. Peak PCA accumulation occurred on day 6 when *RS*Δ12623 produced 2.67 ± 0.08 g/L of PCA in the 4HBA hydrolysates and up to 0.37 ± 0.05 g/L in the wild-type hydrolysates (Fig. 4E). These results suggest that strain *RS*Δ12623 can accumulate low levels of PCA in the absence of 4HBA, which is in agreement with the results observed in rich medium (Fig. 1B). It is worth noting that because of the truncated *p*-coumaric acid degradation pathway, the strain is able to grow on sugars and convert almost all 4HBA to PCA. This enables future strain engineering efforts to redirect more carbon from sugars to PCA instead of cell biomass to potentially reach higher product titers. Additionally, it could be possible to further engineer *RS*Δ12623 to circumvent the catabolic repression by glucose and initiate 4HBA to PCA conversion earlier to reduce fermentation time.

Fermentation scale effects on bioconversion of 4HBA to PCA

To observe the effect of cultivating the strain in a bigger vessel with more controlled conditions compared to shake flasks, *RS*Δ12623 was tested for PCA production at a 2 L bioreactor scale on wild-type and 4HBA hydrolysates generated at the 10 L scale. Foaming during aerobic fermentation of lignocellulosic hydrolysates is a common problem caused by the presence of surface-active agents such as proteins and lipids that are released during the hydrolysis of lignocellulose. To address foaming in aerated 2 L fermentations, a Durasyn 164[52] overlay was added to reduce the surface tension at the gas-liquid interface. Under these conditions, *RS*Δ12623 displayed faster growth and higher glucose and xylose consumption when grown on 4HBA hydrolysates compared to wild-type hydrolysates (Fig. 5A, 5B, and 5C). In both conditions, >95% of the glucose had been consumed after 3 days and >95% of the xylose had been consumed after 5 days. In contrast to shake flask conditions, there was no measured accumulation of PCA by *RS*Δ12623 in wild-type hydrolysates. In 4HBA hydrolysates, after 3 days *RS*Δ12623 had consumed 100% of the available 4HBA and produced 2.28 g/L PCA (Fig. 5D and 5E).

There are marked differences between the flask and 2 L fermentation conditions. The 2 L bioreactors allow for better agitation and oxygen transfer, along with pH control, likely contributing to the cultures reaching their maximum cell density in almost half the time it took in shake flasks (Table 4). Glucose was fully consumed earlier, likely eliminating the catabolic repression of 4HBA consumption, and leading to an earlier PCA production phase in the 2 L conditions compared to the shake flasks. Importantly, both fermentation conditions allowed for the nearly complete consumption of the glucose, xylose, and 4HBA present in the hydrolysates, and in all cases fermentations with *RS*Δ12623 in 4HBA hydrolysates produced close to 100% molar conversion of 4HBA to PCA (Table 5). Interestingly, *RS*Δ12623 accumulated PCA in WT hydrolysates in the flask experiments and generated more PCA than there was 4HBA available in the 2 L reactors. While this accumulation above the levels of 4HBA present could be due to trace amounts of additional upstream metabolites, the accumulation of PCA in rich medium without aromatic supplementation (Fig. 1B) indicates it could be due to the activity of *R. toruloides'* endogenous phenylalanine/tyrosine ammonia-lyase, which can catalyze the conversion of L-tyrosine to *p*-coumaric acid.[53,54] As mentioned before, further engineering of *R. toruloides* to increase carbon flow towards the aromatic biosynthetic pathway from central metabolism could be a promising strategy to increase PCA titers with the biomass conversion process developed in this study.

Table 4. Molecular weight distribution of lignin in solids. Numbers show average ± standard deviation. PDI = polydispersity index.

	Sorghum type	M_w (Da)	M_n (Da)	PDI
Residual solids after pretreatment and saccharification	WT	780 ± 19	235 ± 6	3.3 ± 0.0
	4HBA	749 ± 11	206 ± 5	3.6 ± 0.0
Unreacted solids after depolymerization	WT	1640 ± 125	256 ± 9	6.4 ± 0.3
	4HBA	1036 ± 38	201 ± 4	5.2 ± 0.1

Table 5. Comparison of cultivation times and protocatechuate (PCA) titers and yields, means with the standard deviation when applicable, obtained at different scales for each strain and hydrolysate.

	Shake flasks				**2 L Fermentor**	
Sorghum:*R. toruloides*	WT:WT	WT: *RS*Δ12623	4HBA:WT	4HBA: *RS*Δ12623	WT: *RS*Δ12623	4HBA: *RS*Δ12623
Time until max. OD_{600} (days)	7	7	6	6	3	3
Day 7 glucose utilization (%)	99.75 ± 0.11	99.03 ± 0.25	97.45 ± 0.48	98.41 ± 0.36	99.46	99.74
Day 7 xylose utilization (%)	87.18 ± 0.66	99.16 ± 1.08	82.41 ± 5.90	85.71 ± 0.72	94.63	96.98
Day 7 4HBA utilization (%)	100 ± 0.00	100 ± 0.00	100 ± 0.00	100 ± 0.00	100	100
Max. PCA (g/L)	0	0.41 ± 0.01	0.13 ± 0.11	2.67 ± 0.08	0	2.28
Time until max. PCA (days)	N/A	5	N/A	6	N/A	3
% Yield (mol_{PCA}/mol_{4HBA})	N/A	N/A	4.95%	95.86%	N/A	107.68%

Conclusions

Overall, this work showcases the potential of combining engineered plants enriched for critical precursors with microbes capable of converting them at high yields to desirable compounds. While different bioproducts have previously been produced from [Ch][Lys] derived hydrolysates, this is the first time that aromatic precursors were purposefully produced *in planta* and liberated during the pretreatment and enzymatic hydrolysis stages for subsequent microbial conversion after minimal hydrolysate conditioning. Here we produce PCA almost entirely from the 4HBA in the enriched hydrolysates, eliminating the need to supplement the feedstock with costly carbon sources, such as purified sugars or additional aromatics, as other studies do. The titers we achieved were possible because the amount of 4HBA in the engineered sorghum was significantly higher than what is observed in non-engineered plants. Further increasing 4HBA production in the plant and the development of a process to efficiently release *p*-coumaric acid should directly translate to higher PCA titers under the conditions tested here. The PCA produced in this study can further be connected to multiple downstream processes and this study lays the foundation for future efforts to efficiently convert engineered plants to bioproducts using engineered microbes and greener biocompatible solvents such as cholinium-based ionic liquids.

Author Contributions

V.E.G., V.P. C.A.B, D.L, P.O, O.W., H.C., N.S, A.E., E.S., H.V.S., D.H.P., A.M., B.A.S, J.M.G., and A.R. designed the research; V.E.G, V.P., C.A.B., D.L., P.O., O.W., and H.C. performed the experiments and analyzed the data; V.E.G., V.P., D.L., and A.R. wrote the paper; all authors reviewed and edited the manuscript.

Conflicts of interest

B.A.S has a financial interest in Caribou Biofuels and Illium Technologies. HC, BAS, and JMG are named inventors on at least one related patent filing.

Acknowledgements

The authors would like to thank Asun Oka and Chien-Yuan Lin for technical and intellectual support and Corinne Scown,

Steven Singer, Deepti Tanjore, Jenny Mortimer, Robert Hutmacher, and Taek Soon Lee for fruitful discussions. This work was supported by the DOE Joint BioEnergy Institute supported by the U.S. Department of Energy, Office of Science, Office of Biological and Environmental Research, through contract DE-AC02-05CH11231 between Lawrence Berkeley National Laboratory and the U.S. Department of Energy. The United States Government retains and the publisher, by accepting the article for publication, acknowledges that the United States Government retains a non-exclusive, paid-up, irrevocable, worldwide license to publish or reproduce the published form of this manuscript, or allow others to do so, for United States Government purposes. The Department of Energy will provide public access to these results of federally sponsored research in accordance with the DOE Public Access Plan. Sandia National Laboratories is a multimission laboratory managed and operated by National Technology & Engineering Solutions of Sandia, LLC, a wholly owned subsidiary of Honeywell International Inc., for the U.S. Department of Energy's National Nuclear Security Administration under contract DE-NA0003525. This paper describes objective technical results and analysis. Any subjective views or opinions that might be expressed in the paper do not necessarily represent the views of the U.S. Department of Energy or the United States Government.

Notes and references

1 B. F. Pfleger and R. Takors, *Curr. Opin. Biotechnol.*, 2023, **80**, 102913.

2 J. Montaño López, L. Duran and J. L. Avalos, *Nat. Rev. Microbiol.*, 2022, **20**, 35–48.

3 H. Lu, V. Yadav, M. Bilal and H. M. N. Iqbal, *Chemosphere*, 2022, **288**, 132574.

4 N. R. Baral, E. R. Sundstrom, L. Das, J. M. Gladden, A. Eudes, J. Mortimer, S. W. Singer, A. Mukhopadhyay and C. D. Scown, *ACS Sustain. Chem. Eng.*, 2019, **7**, 9062–9079.

5 K. Kucharska, P. Rybarczyk, I. Hołowacz, R. Łukajtis, M. Glinka and M. Kamiński, *Molecules*, 2018, **23**, 2937. DOI:10.3390/molecules23112937.

6 A. R. Mankar, A. Pandey, A. Modak and K. K. Pant, *Bioresour. Technol.*, 2021, **334**, 125235.

7 A. Lorenci Woiciechowski, C. J. Dalmas Neto, L. Porto de Souza Vandenberghe, D. P. de Carvalho Neto, A. C. Novak Sydney, L. A. J. Letti, S. G. Karp, L. A. Zevallos Torres and C. R. Soccol, *Bioresour. Technol.*, 2020, **304**, 122848.

8 J. Ralph, C. Lapierre and W. Boerjan, *Curr. Opin. Biotechnol.*, 2019, **56**, 240–249.

9 H. Wang, Y. Pu, A. Ragauskas and B. Yang, *Bioresour. Technol.*, 2019, **271**, 449–461.

10 Y. Suzuki, Y. Okamura-Abe, Y. Otsuka, T. Araki, M. Nojiri, N. Kamimura, E. Masai and M. Nakamura, *Bioresour. Technol.*, 2022, **363**, 127836.

11 S. D. Karlen, P. Fasahati, M. Mazaheri, J. Serate, R. A. Smith, S. Sirobhushanam, M. Chen, V. I. Tymokhin, C. L. Cass, S. Liu, D. Padmakshan, D. Xie, Y. Zhang, M. A. McGee, J. D. Russell, J. J. Coon, H. F. Kaeppler, N. de Leon, C. T. Maravelias, T. M. Runge, S. M. Kaeppler, J. C. Sedbrook and J. Ralph, *ChemSusChem*, 2020, **13**, 2012–2024.

12 J. Mullet, D. Morishige, R. McCormick, S. Truong, J. Hilley, B. McKinley, R. Anderson, S. N. Olson and W. Rooney, *J. Exp. Bot.*, 2014, **65**, 3479–3489.

13 K. Markel, M. S. Belcher and P. M. Shih, *Curr. Opin. Biotechnol.*, 2020, **62**, 196–201.

14 Y. Mottiar, R. Vanholme, W. Boerjan, J. Ralph and S. D. Mansfield, *Curr. Opin. Biotechnol.*, 2016, **37**, 190–200.

15 M. Yang, D. Liu, N. R. Baral, C.-Y. Lin, B. A. Simmons, J. M. Gladden, A. Eudes and C. D. Scown, *Proc Natl Acad Sci USA*, 2022, **119**, e2122309119.

16 C. Kempinski, Z. Jiang, G. Zinck, S. J. Sato, Z. Ge, T. E. Clemente and J. Chappell, *Plant Biotechnol. J.*, 2019, **17**, 373–385.

17 Z. Wen, S. Zhang, C. K. Odoh, M. Jin and Z. K. Zhao, *FEMS Yeast Res.*, 2020, **20**, 5.

18 J. Yaegashi, J. Kirby, M. Ito, J. Sun, T. Dutta, M. Mirsiaghi, E. R. Sundstrom, A. Rodriguez, E. Baidoo, D. Tanjore, T. Pray, K. Sale, S. Singh, J. D. Keasling, B. A. Simmons, S. W. Singer, J. K. Magnuson, A. P. Arkin, J. M. Skerker and J. M. Gladden, *Biotechnol. Biofuels*, 2017, **10**, 241.

19 Y.-K. Park, J.-M. Nicaud and R. Ledesma-Amaro, *Trends Biotechnol.*, 2018, **36**, 304–317.

20 J. Kirby, G. M. Geiselman, J. Yaegashi, J. Kim, X. Zhuang, M. B. Tran-Gyamfi, J.-P. Prahl, E. R. Sundstrom, Y. Gao, N. Munoz, K. E. Burnum-Johnson, V. T. Benites, E. E. K. Baidoo, A. Fuhrmann, K. Seibel, B.-J. M. Webb-Robertson, J. Zucker, C. D. Nicora, D. Tanjore, J. K. Magnuson, J. M. Skerker and J. M. Gladden, *Biotechnol. Biofuels*, 2021, **14**, 101.

21 P. B. Otoupal, G. M. Geiselman, A. M. Oka, C. A. Barcelos, H. Choudhary, D. Dinh, W. Zhong, H. Hwang, J. D. Keasling, A. Mukhopadhyay, E. Sundstrom, R. W. Haushalter, N. Sun, B. A. Simmons and J. M. Gladden, *Microb. Cell Fact.*, 2022, **21**, 254.

22 J. Kim, S. T. Coradetti, Y.-M. Kim, Y. Gao, J. Yaegashi, J. D. Zucker, N. Munoz, E. M. Zink, K. E. Burnum-Johnson, S. E. Baker, B. A. Simmons, J. M. Skerker, J. M. Gladden and J. K. Magnuson, *Front. Bioeng. Biotechnol.*, 2020, **8**, 612832.

23 D.-H. Jung, E.-J. Kim, E. Jung, R. J. Kazlauskas, K.-Y. Choi and B.-G. Kim, *Biotechnol. Bioeng.*, 2016, **113**, 1493–1503.

24 J. L. Torres Y Torres and J. P. Rosazza, *J. Nat. Prod.*, 2001, **64**, 1408–1414.

25 P. Calero, S. I. Jensen, K. Bojanovič, R. M. Lennen, A. Koza and A. T. Nielsen, *Biotechnol. Bioeng.*, 2018, **115**, 762–774.

26 K. Krzysztoforska, D. Mirowska-Guzel and E. Widy-Tyszkiewicz, *Nutr. Neurosci.*, 2019, **22**, 72–82.

27 S. Kakkar and S. Bais, *ISRN Pharmacol.*, 2014, **2014**, 952943.

28 N. A. Rorrer, S. F. Notonier, B. C. Knott, B. A. Black, A. Singh, S. R. Nicholson, C. P. Kinchin, G. P. Schmidt, A. C. Carpenter,

K. J. Ramirez, C. W. Johnson, D. Salvachúa, M. F. Crowley and G. T. Beckham, *Cell Reports Physical Science*, 2022, **3**, 100840.

29 J. Song, Y. He, C. Luo, B. Feng, F. Ran, H. Xu, Z. Ci, R. Xu, L. Han and D. Zhang, *Pharmacol. Res.*, 2020, **161**, 105109.

30 Y. Okamura-Abe, T. Abe, K. Nishimura, Y. Kawata, K. Sato-Izawa, Y. Otsuka, M. Nakamura, S. Kajita, E. Masai, T. Sonoki and Y. Katayama, *J. Biosci. Bioeng.*, 2016, **121**, 652–658.

31 W. Wu, T. Dutta, A. M. Varman, A. Eudes, B. Manalansan, D. Loqué and S. Singh, *Sci. Rep.*, 2017, **7**, 8420.

32 C. W. Johnson, D. Salvachúa, N. A. Rorrer, B. A. Black, D. R. Vardon, P. C. St. John, N. S. Cleveland, G. Dominick, J. R. Elmore, N. Grundl, P. Khanna, C. R. Martinez, W. E. Michener, D. J. Peterson, K. J. Ramirez, P. Singh, T. A. VanderWall, A. N. Wilson, X. Yi, M. J. Biddy, Y. J. Bomble, A. M. Guss and G. T. Beckham, *Joule*, 2019, **3**, 1526-1537.

33 M. Labib, J. Görtz, C. Brüsseler, N. Kallscheuer, J. Gätgens, A. Jupke, J. Marienhagen and S. Noack, *Biotechnol. Bioeng.*, 2021, **118**, 4414–4427.

34 J. Li and B.-C. Ye, *Bioresour. Technol.*, 2021, **319**, 124239.

35 J. Zhang, X. Zhang, M. Yang, S. Singh and G. Cheng, *Bioresour. Technol.*, 2021, **322**, 124522.

36 H. D. Magurudeniya, N. R. Baral, A. Rodriguez, C. D. Scown, J. Dahlberg, D. Putnam, A. George, B. A. Simmons and J. M. Gladden, *Green Chem.*, 2021, **23**, 3127–3140.

37 C.-Y. Lin, Y. Tian, K. Nelson-Vasilchik, J. Hague, R. Kakumanu, M. Y. Lee, V. R. Pidatala, J. Trinh, C. M. De Ben, J. Dalton, T. R. Northen, E. E. K. Baidoo, B. A. Simmons, J. M. Gladden, C. D. Scown, D. H. Putnam, A. P. Kausch, H. V. Scheller and A. Eudes, *Metab. Eng. Commun.*, 2022, **15**, e00207.

38 A. Sluiter, B. Hames, R. Ruiz, C. Scarlata, J. Sluiter, D. Templeton and D. Crocker, *Determination of structural carbohydrates and lignin in biomass. Laboratory analytical procedure.*, NREL, 2008.

39 J. L. Gardner, W. He, C. Li, J. Wong, K. L. Sale, B. A. Simmons, S. Singh and D. Tanjore, *RSC Adv.*, 2015, **5**, 51092–51101.

40 H. Choudhary, L. Das, J. G. Pelton, L. Sheps, B. A. Simmons, J. M. Gladden and S. Singh, *Chem. Eur. J*, 2023, **29**, e202300330.

41 R. Chari, N. C. Yeo, A. Chavez and G. M. Church, *ACS Synth. Biol.*, 2017, **6**, 902–904.

42 A. Rodriguez, N. Ersig, G. M. Geiselman, K. Seibel, B. A. Simmons, J. K. Magnuson, A. Eudes and J. M. Gladden, *Bioresour. Technol.*, 2019, **286**, 121365.

43 H. Ren, M.-H. Zong, H. Wu and N. Li, *ACS Sustain. Chem. Eng.*, 2016, **4**, 5659–5666.

44 V. Rigual, G. Papa, A. Rodriguez, M. Wehrs, K. H. Kim, M. Oliet, M. V. Alonso, J. M. Gladden, A. Mukhopadhyay, B. A. Simmons and S. Singh, *ACS Sustain. Chem. Eng.*, 2020, **8**, 836-856.

45 V. Jassal, C. Dou, N. Sun, S. Singh, B. A. Simmons and H. Choudhary, *Front. Chem. Eng.*, 2022, **4**, 1059305.

46 A. Tolbert, H. Akinosho, R. Khunsupat, A. K. Naskar and A. J. Ragauskas, *Biofuels, Bioprod. Bioref.*, 2014, **8**, 836–856.

47 M. Wehrs, J. M. Gladden, Y. Liu, L. Platz, J.-P. Prahl, J. Moon, G. Papa, E. Sundstrom, G. M. Geiselman, D. Tanjore, J. D. Keasling, T. R. Pray, B. A. Simmons and A. Mukhopadhyay, *Green Chem.*, 2019, **21**, 3394–3406.

48 E. Sundstrom, J. Yaegashi, J. Yan, F. Masson, G. Papa, A. Rodriguez, M. Mirsiaghi, L. Liang, Q. He, D. Tanjore, T. R. Pray, S. Singh, B. Simmons, N. Sun, J. Magnuson and J. Gladden, *Green Chem.*, 2018, **20**, 2870–2879.

49 H. Ronne, *Trends Genet.*, 1995, **11**, 12–17.

50 S. Dal, I. Steiner and U. Gerischer, *J. Mol. Microbiol. Biotechnol.*, 2002, **4**, 389–404.

51 M. R. Mäkelä, M. V. Aguilar-Pontes, D. van Rossen-Uffink, M. Peng and R. P. de Vries, *Sci. Rep.*, 2018, **8**, 6655.

52 Information | Information | INEOS Oligomers, https://www.ineos.com/businesses/ineos-oligomers/products/durasyn-polyalphaolefin-pao/, (accessed March 27, 2023).

53 M. Zhang, Q. Gao, Y. Liu, Z. Fang, Z. Gong, Z. K. Zhao and X. Yang, *Microb. Cell Fact.*, 2022, **21**, 270.

54 O. Adachi, K. Matsushita, E. Shinagawa and M. Ameyama, *Agric. Biol. Chem.*, 1990, **54**, 2839–2843.

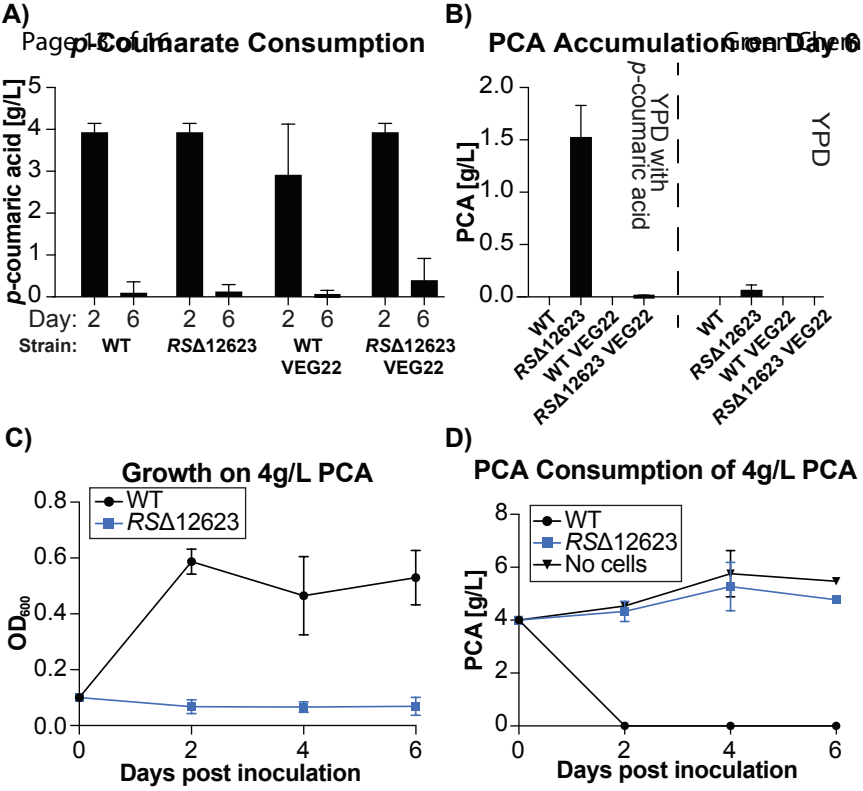

Figure 1. Characterization of the accumulation and consumption of PCA by wild-type R. toruloides and RSΔ12623. A) p-Coumaric acid levels at the start of fermentation and at day 6 for wild-type (WT), RSΔ12623, wild-type transformed with VEG22 containing a wild-type copy of RTO4_12623 (WT VEG22), and RSΔ 12623 transformed with VEG22 containing a wild-type copy of RTO4_12623 (RSΔ 12623 VEG22). B) PCA concentrations at day 6 of the fermentation with the same strains as panel A in YPD with or without 4 g/L p-coumaric acid. C) Growth of WT and RSΔ12623 strains in YNB with 4 g/L PCA as the sole carbon source. D) PCA concentrations after incubation of WT and RSΔ12623 strains in YNB with 4 g/L PCA as the sole carbon source and an uninoculated control. Experiments for A and B were performed three times in triplicate. Experiments for C and D were performed twice in triplicate. Bars and points represent the mean across experiments and the error bars represent the standard deviations.

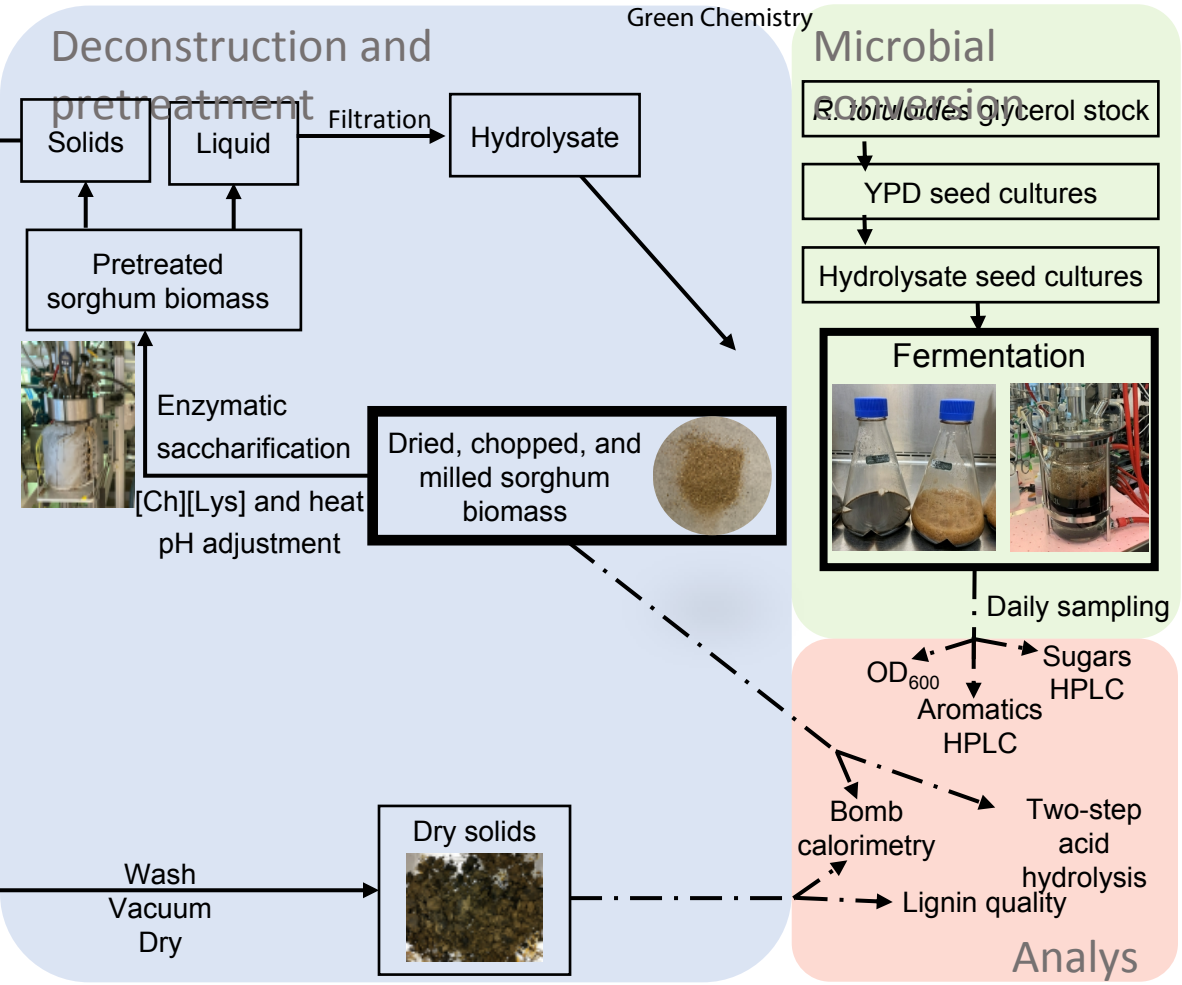

Figure 2. Scheme of the reactions employed for hydrolysate generation, characterization of the liquid and solid fractions and fermentation, using wild-type or 4HBA sorghum biomass.

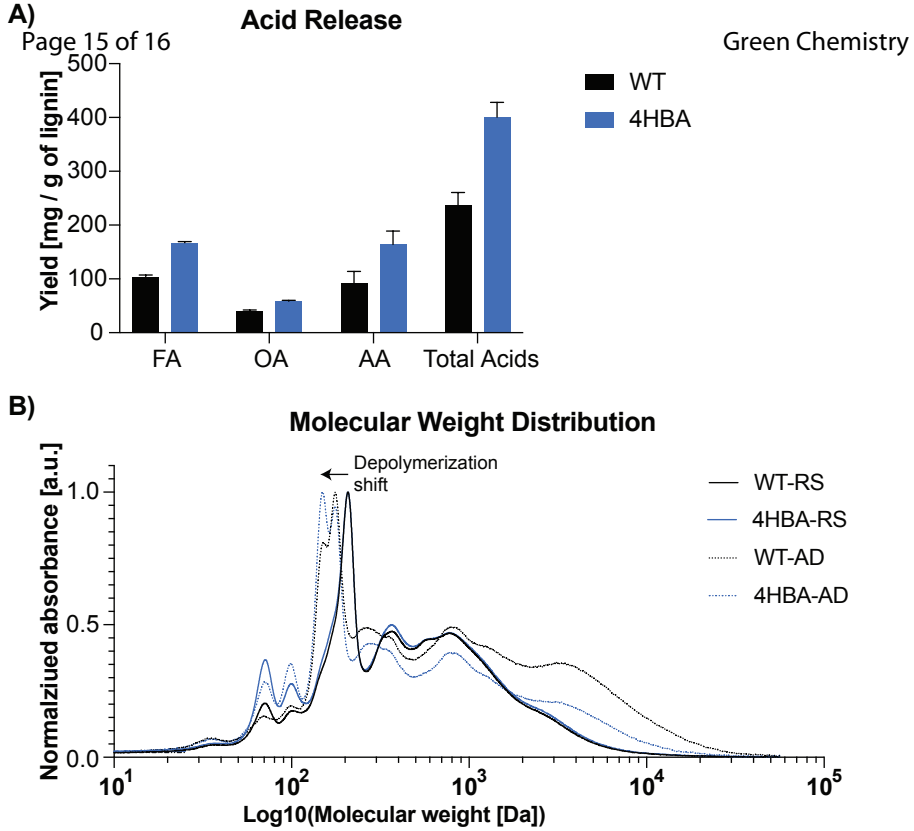

Figure 3. Analysis of the recovered lignin after pretreatment and enzymatic saccharification to determine suitability to further chemical depolymerization. A) Mean molecular weight distribution of lignin in residual solids before and after lignin depolymerization chemistry with error bars representing the standard deviation. B) Yields of acids generated in the lignin depolymerization reaction. FA = formic acid, OA = oxalic acid, AA = acetic acid. WT-RS and 4HBA-RS represent the residual solids after pretreatment and saccharification obtained from wild-type and 4HBA biomasses, respectively. WT-AD and 4HBA-AD represent the materials WT-RS and 4HBA-RS after lignin depolymerization.

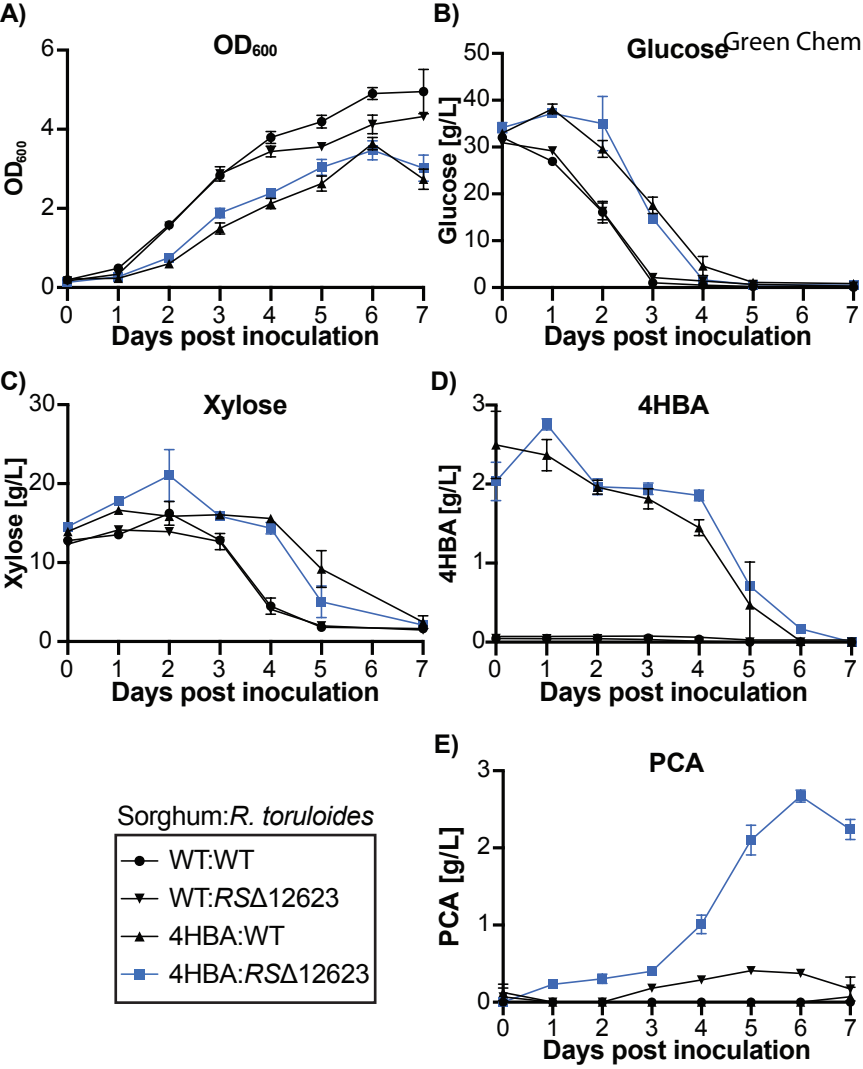

Figure 4. 25mL shake flask cultivations of wild-type (WT) R. toruloides and RSΔ12623 on wild-type (WT) or 4HBA sorghum hydrolysates. A) Cell density (OD600), B) Glucose concentration, C) Xylose concentration, D) 4HBA concentration, E) PCA concentration. The points represent the mean of three replicates, and the error bars represent the standard deviation.

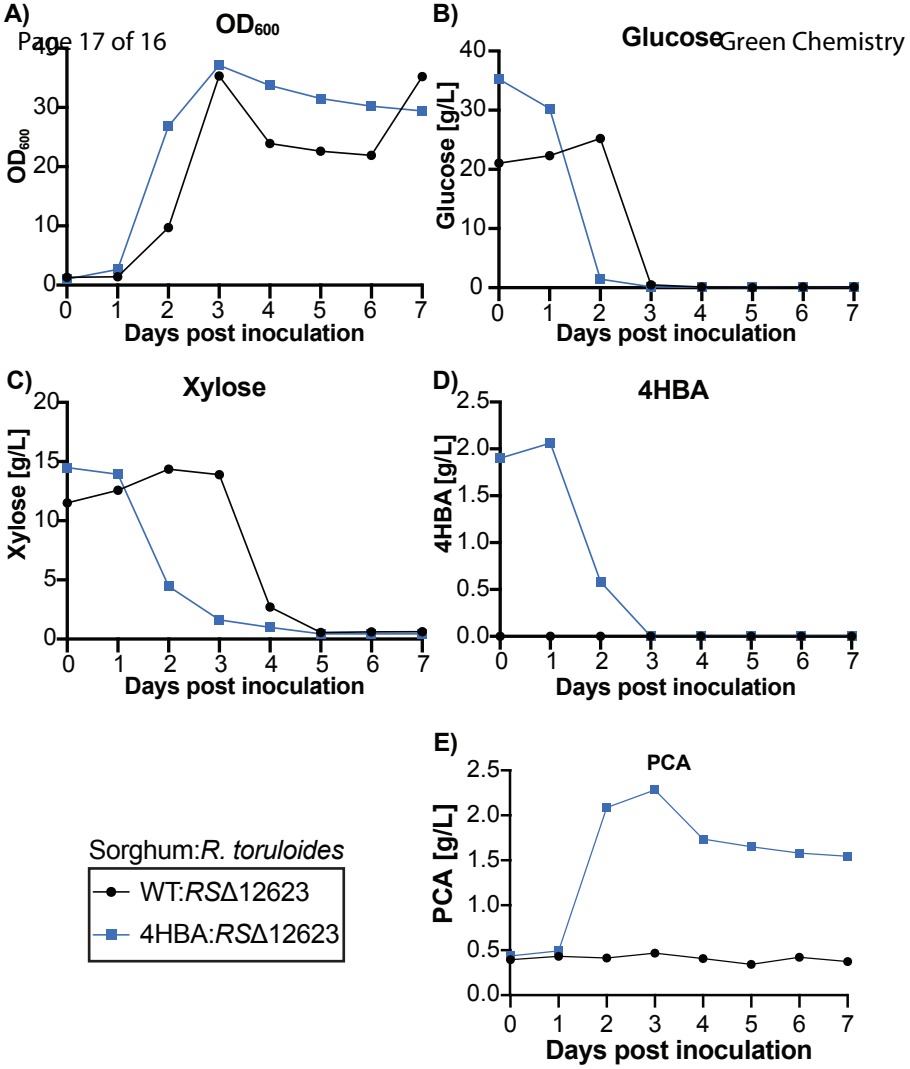

Figure 5. Bioreactor cultivations of wild-type (WT) and PCA producing R. toruloides grown on either wild-type (WT) or 4HBA-enriched sorghum hydrolysates for 5 d in singlicate. A) Cell density (OD600), B) Glucose concentration, C) Xylose concentration, D) 4HBA concentration, E) PCA concentration. The vessel volume was 2 L and the working volume was 1.25 L.